12 Annual Conference of the Materials Research Society of Serbia, Herceg Novi, Montenegro, September 6–10, 2010

Structure Prediction for PbS and ZnO at Different Pressures and Visualization of the Energy Landscapes

D. Zagorac*, J.C. Schön, K. Doll and M. Jansen

Max Planck Institute for Solid State Research, Heisenbergstraße 1, D-70569 Stuttgart, Germany

An important issue in modern solid state chemistry is the development of a general methodology to predict the possible (meta)-stable modifications of a solid. This requires the global exploration of the energy landscape of the chemical system, since each stable phase corresponds to a locally ergodic region of the landscape. The global search in the lead sulfide system has been performed with simulated annealing on the ab initio level, while zinc oxide was studied with an empirical potential using simulated annealing, both at standard and elevated pressure (up to 100 GPa). The local optimization of the modifications found in the PbS system was performed using various density functionals. Next, the energy $E(V)$ and enthalpy $H(p)$ as function of volume and pressure, respectively, were computed for these modifications and their electronic structure was analyzed. The structures found for ZnO were locally optimized on ab initio level (DFT and Hartree-Fock). In both systems the structures found were in good agreement with the experiment. Furthermore, we employed the threshold algorithm to explore the barrier structure of the landscape of ZnO as function of the number of formula units in the simulation cell. Based on the barrier and minima information 2-D models of the energy landscape were constructed.

PACS: 61.50Ah, 61.66Fn, 61.50Ks, 71.50Nc

1. Introduction

The search for new crystalline compounds is a central topic of solid state chemistry. Scientists have successfully synthesized many new materials and studied their properties, but the purely experimental approach is no longer the only route to discover new compounds. The theoretical prediction of new compounds and new (meta)-stable modifications of already existing solids followed by their synthesis is fast becoming an alternative [1–10].

Conceptually, this requires a global exploration of the energy landscape of the chemical system of interest [1, 4, 11], since each stable phase corresponds to a locally ergodic region of the landscape. While for many ionic systems, such as TiO_2 [12], $MgSiO_3$ [13], halides [14], and sulfides of the alkali metals [15], or the earth alkaline halides [16] and oxides [17, 18], the most important modifications can be identified using an empirical potential energy landscape, this is no longer true for systems with covalent bonds, complex ions, or non-bonding electron pairs. For such systems, the energy calculation during the global optimization must be performed on the ab initio level [9, 19–23]. As an example, we have studied PbS, where steric electron pairs may play a role.

In order to gain a deeper insight into the structural relations of a chemical system and the kinetic stability of the meta-stable compounds, it is becoming increasingly important to develop new methods for analyzing and representing the barrier structure of energy landscapes. One of the main problems lies in the visualization of a high-dimensional space, and in the complexity of the landscape. Thus, finding low-dimensional representations of the energy landscape, which can help to analyze specific landscape features, would be a significant step. In the second part of this study, we analyze the energy landscape of ZnO at the empirical potential level, and present several ways to depict static and dynamic features of the landscape.

2. Methods

Our general approach to the determination of structure candidates has been given in detail elsewhere [1, 8, 9], here we will just outline the main steps of the method and provide information specific to this investigation. The (meta)stable phases capable of existence correspond to locally ergodic regions on the enthalpy landscape of the chemical system of interest. At low temperatures, these regions are basins around local minima of the potential energy, while at elevated temperatures locally ergodic regions can encompass many (often structurally related) local minima [5]. These minima are identified using simulated annealing (SA) [24], usually with up to 4 formula units/simulation cell, where both atom positions and cell parameters can be freely varied without any symmetry constraints. Energy barriers are determined using the threshold algorithm (TA) [25], where the landscape accessible from a local minimum below a sequence of energy

* corresponding author; e-mail: d.zagorac@fkf.mpg.de

barriers (thresholds) is systematically explored for all important local minima. In particular, we can measure the transition probability among the minima as a function of the threshold value (c.f. Fig. 6).

During the global optimization, the energy calculation is performed at the ab-initio level or using empirical potentials. In order to be able to rank the various modifications found, all structures are refined using both Hartree-Fock and DFT-based ab-initio energy minimizations. From the computed $E(V)$ (energy as fuction of volume) and $H(p)$ (enthalpy as function of pressure) curves, one then derives the transition pressures between the thermodynamically stable modifications. Since there is usually a very large number of structure candidates, this refinement is often automatically performed with a heuristic algorithm [15].

Furthermore the symmetries and space groups of the configurations are determined using the algorithms SFND (Symmetry FiNDer) [26] and RGS (Raum Gruppen Suchen = Space group search) [27], and the CMPZ (CoMPare Zelle = Compare cells) algorithm is used to eliminate duplicate structures [28]. We note that these symmetries allow us to propose possible transformation paths among different modifications, just as the principal coordinates hint at paths for transitions in large molecules. But one should be aware that with the exception of second order phase transitions one cannot expect that the simple "straightforward" path one would construct based on symmetry considerations, corresponds to the actual route on the landscape taken during the phase transformation.

In addition to the TA runs, we also perform prescribed path (PP) studies when analyzing structures and the barriers of the landscape. This algorithm is related to the nudged elastic band (NEB) method [29], and is employed for finding saddle regions and minimum energy paths between various locally ergodic regions. The method works by optimizing the atom arrangement at a number of intermediate steps along a "reaction path" (c.f. Fig. 1). At each step one finds the lowest energy configuration while maintaining the value of the "reaction coordinate".

Like the NEB method, the PP algorithm allows a defined number of steps along a well-defined route or within a well-defined set (e.g. varying atom positions and / or cell parameters) of possible downhill moves (e.g. gradient descent or stochastic quench). The prescribed path algorithm allows us additionally to perform a Monte Carlo simulation at a given temperature for each local run orthogonal to the path defined, before the local minimization takes place. This allows us to cross small barriers in the direction orthogonal to the "reaction coordinate". Note that in contrast to the classical NEB-method, the relaxation during the PP-runs can yield several nearby relaxed paths, competing with each other. Thus the "transition route" associated with one given prescribed path can consist of a bundle of similar but different individual transition paths.

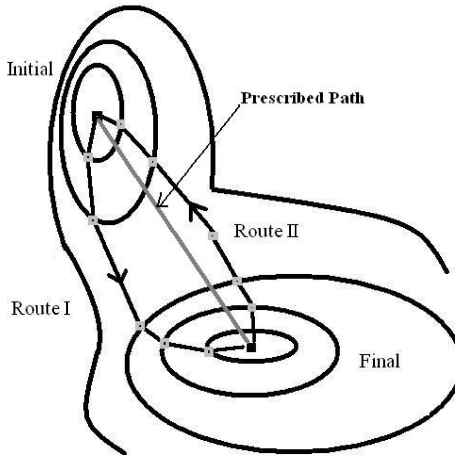

Fig. 1. Schematic PP algorithm based model: 2 minima are connected in a high dimensional space via a prescribed path, but starting from this path they can find different routes to relax to.

3. Examples

As an example system for ab initio global exploration, we have chosen lead sulfide (see 3.1), and for a global search with an empirical potential we have chosen zinc oxide (see 3.2), respectively.

3.1. Lead sulfide (PbS)

Lead sulfide is used as a detection material in various infra-red sensors (photon detectors) [30]. However, the high dielectric constant of PbS leads to relatively slow detectors, compared to silicon, germanium, InSb, or HgCdTe. Clearly, identifying (and eventually synthesizing) a new PbS-modification with improved properties would be very useful.

Under standard conditions, the experimentally known modification of lead sulfide crystallizes in the NaCl structure type (B1) [31]. PbS undergoes a pressure-induced phase transition from the NaCl (B1) type to an intermediate orthorhombic phase (suggested to belong to the B16 or B33 structure types at 2.2 GPa [32–34]. A further pressure-induced phase transition from the orthorhombic phase to the CsCl type (B2) phase takes place at 21.5 GPa [32]. However, the experimental data do not fully clarify the properties of the intermediate orthorhombic phase.

We performed a structure prediction study for bulk PbS at different pressures (0–24 GPa) using ab initio energy calculations during both the global search and the local optimization. According to our calculations we find a transition from the NaCl type to the thallium iodide (B33) type at 4.5 GPa, which is in agreement with what is found in the experiment [32, 33]. Also, we discovered a new competitive orthorhombic phase, showing the iron boride (B27) type, which appears at a slightly higher pressure than the TlI type. This may help to clarify the experimental data, where an up-to-now unidentified

orthorhombic phase has been claimed to exist at intermediary pressures [35]. Furthermore the TlI (FeB) to CsCl transition was observed at 25 GPa, and again this is in agreement with experiment. We have found new structure candidates which have not yet been discussed theoretically or experimentally, in particular two additional modifications exhibiting the GeTe-structure type (c.f. Fig. 2) and the wurtzite type, respectively, which might be stable at slightly negative pressures. Additional promising meta-stable phases found exhibited the tungsten carbide (WC) type and nickel arsenide (NiAs) type of structure at ambient conditions, and at elevated pressures some unknown structure types labeled PbS I-III [36]. Furthermore, we have investigated the charge densities and electronic band structures of the most relevant compounds, which appeared to be in good agreement with experimental information.

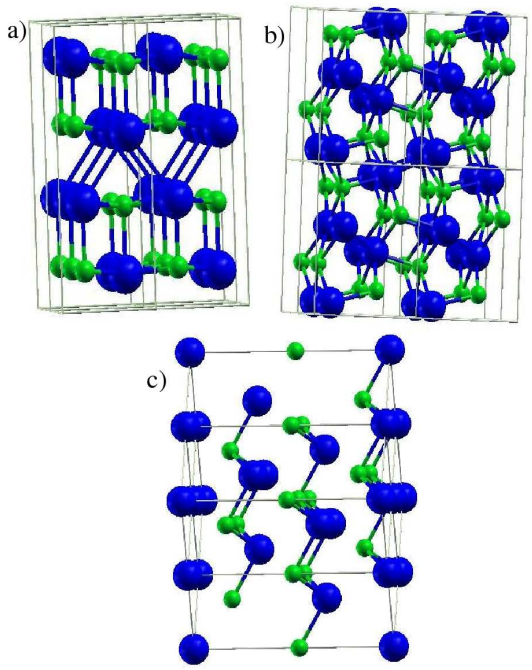

Fig. 2. Visualisation of structure types found in PbS system: a) TlI-type; b) FeB-type; c) GeTe-type (Small light spheres and large dark spheres correspond to S and Pb atoms, respectively).

3.2. Zinc oxide (ZnO)

In materials science, ZnO is known as a II–VI semiconductor with several favorable properties: good transparency, high electron mobility, wide bandgap, strong room-temperature luminescence, etc. Due to these properties, ZnO is already used in emerging applications for transparent electrodes in liquid crystal displays and in energy-saving or heat-protecting windows. ZnO powder is widely used as an additive to numerous materials and products including plastics, ceramics, glass, cement, rubber, oil lubricants, paints, adhesives, sealants, pigments, foods (source of Zn nutrient), batteries, etc [37].

Bulk zinc oxide is known to crystallize in three structure types: hexagonal wurtzite, cubic sphalerite (ZnS) and cubic rocksalt (NaCl) [38, 39]. The wurtzite structure is the most stable one at ambient conditions and thus most common. The sphalerite modification can be stabilized by growing ZnO on substrates with cubic lattice structure, while the rocksalt (NaCl) structure is only observed at relatively high pressures above 10 GPa [40].

Since there are only three confirmed experimentally observed forms of ZnO, finding new polymorphs and understanding transitions among them would be very important. Thus, when exploring the energy landscape of ZnO, we determine new modifications, investigate the relations between them, and study the influence of pressure and temperature in the system.

We globally explored the zinc oxide system with an empirical potential (Coulomb + Lennard-Jones potential) using simulated annealing, both at standard and elevated pressure (up to 100 GPa). The local optimization was performed using Hartree-Fock and various density functionals (LDA and B3LYP). After the global and local optimizations were finished, a full analysis of the energy landscape of the system was performed with the threshold algorithm for different numbers of formula units per simulation cell. A particular focus of this study was the investigation of the barrier structure in more detail, e.g. taking into account the fact that an infinite periodic structure can be represented by many different finite unit cells, each corresponding to a different local minimum on the energy landscape being explored.

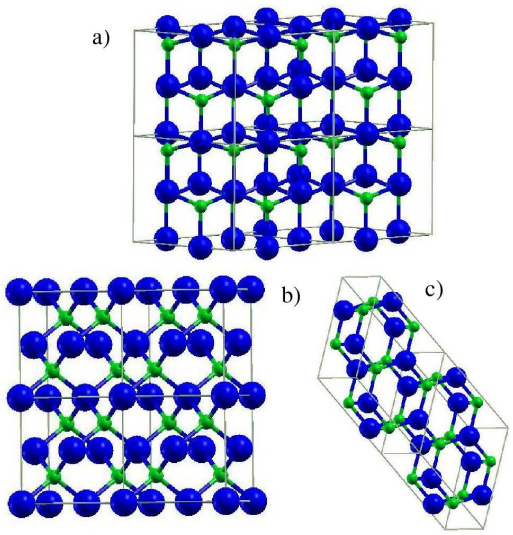

Fig. 3. Visualization of structure types found in ZnO system: a) wurtzite-type; b) sphalerite-type; c) 5-5 type (Zn^- and O^- ions are coordinated by trigonal bipyramids of O^- and Zn^- ions, respectively). Small light spheres and large dark spheres correspond to O and Zn atoms, respectively).

Our calculations confirm that the experimentally observed polymorphs of zinc oxide are the energetically lowest and thermodynamically most stable ones. We have found some new hypothetical modifications in the ZnO system, exhibiting the nickel-arsenide (NiAs) type and the β-BeO-type. One further interesting structure candidate, which we found as a metastable phase along the route of the wurtzite-NaCl transition is the so called "5-5"type [41] (c.f. Fig. 3), the existence of which has been postulated in some recent experiments [42, 43].

Regarding the barrier structure of the energy landscape, wurtzite and sphalerite appear to exhibit the largest barriers and thus the highest kinetic stability. We note that there exist noticeable energy barriers between different representations of a given periodic structure. These barriers would be especially relevant, and might pose serious problems, for the interpretation of molecular dynamics based explorations of the landscape; when using Monte Carlo methods, these barriers can (in principle) be eliminated by performing large moves in cell parameter space.

4. Visualization techniques in energy landscapes representation

When using energy landscapes to understand the behavior of chemical systems, one faces the formidable problem that the landscapes are high-dimensional and possess very complicated barrier structures. Finding low-dimensional representations of the energy landscape and analyzing its features would give us new insights about the specific system. For a small molecule, or molecules consisting of a few essentially rigid building blocks, one can employ low-dimensional projections of the landscape to highlight important features of e.g. the transition path during a conformational change or a chemical reaction [44]. For larger molecules, finding reduced coordinates has led to the application of the so-called principal coordinate analysis (PCA) to the configurations that represent local minima [45]. For solids, this approach appears to be most suited for amorphous or glassy compounds, where large classes of similar dynamically relevant minima exist.

In order to represent our results in solid state chemistry problems, we must reduce the high dimensionality of the energy landscape (EL). Several closely related graph based methods are already known from the literature, tree graph, disconnectivity graph, lumped graph or 1d-projection [11, 25, 46, 47]. All of these methods yield a 1-dimensional picture of the EL and are based on the same basic idea (start from one local minimum, select an energy lid, observe allowed transitions between minima, and then repeat with a higher lid, till all the minima on the landscape are connected). Recent variations taking some additional information into account are e.g. the alternative disconnectivity graph [48] or topology networks [49].

Since these one-dimensional representations of the EL are well known types of visualization, we present instead new 2-D models of the ZnO landscsape. In Fig. 4 we focus on a subregion containing only two minima of the landscape. In both cases, the x-coordinate corresponds to the volume per 2 formula units of ZnO. In Fig. 4a the y-coordinate is the cell parameter a, and in Fig 4b, y corresponds to the average distance value (R). R is calculated as the mean of all distances within the first neighbor sphere of the atoms in the configurations represented in the model. Based on the data points calculated with the PP-algorithm (c.f. Fig. 5.), the projected landscape between these points has been interpolated using a special topological MatLab tool (biharmonic spline interpolation) [50].

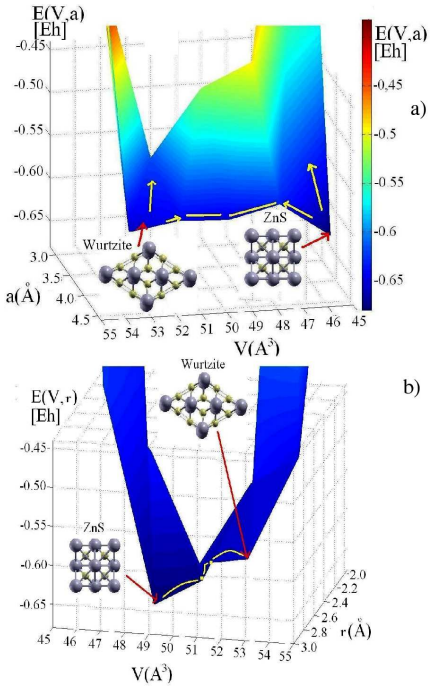

Fig. 4. Models of the energy landscape of ZnO based on PP-algorithm runs, using sphalerite/wurtzite as initial/final configurations with 2 formula unit/simulation cell. x-coordinate = volume, y-coordinate = a-parameter of the crystallographic cell (a)) or average atom-atom nearest neighbor distances (b)), z-coordinate = energy.

Another important aspect of the landscape are the probability flows between the minima which directly reflect the relaxation and transformation dynamics. While the actual flows will depend on the temperature, of course, important information is already contained in the observed transition probabilities as function of energy lid during the threshold runs. These probabilities can be represented in a transition map [51], where the major basins of the energy landscape are depicted, together with connections showing the amount of probability flow as function of energy range. We show here one of the TA probability graphs for the flow emanating from the sphalerite minimum (denoted ZnS) as function of energy

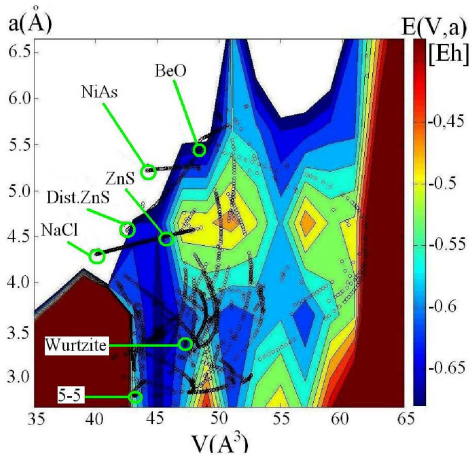

Fig. 5. Model using all relevant local minima as initial/final configuration (sphalerite, wurtzite, 5-5, NaCl, NiAs and BeO type). Points correspond to the restricted minima (for given V and a) found on the EL with PP-algorithm.

lid (c.f. Fig. 6.). By combining the graphs for all starting minima with local densities of states measured by the threshold algorithm, one can (in principle) construct a temperature dependent probability Markov matrix describing the relaxation dynamics on the landscape.

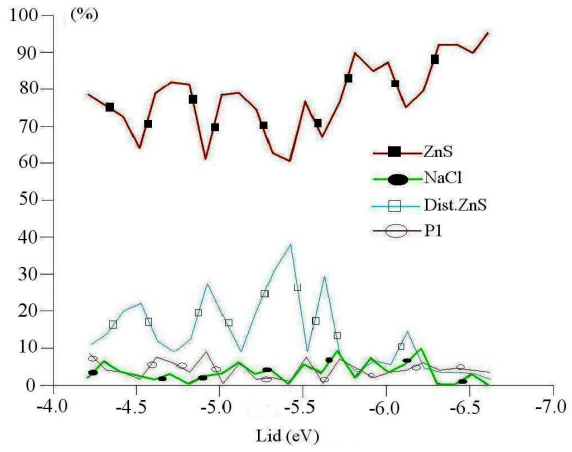

Fig. 6. TA probability graph in ZnO system with 1 formula unit/simulation cell (sphalerite is chosen as starting point). We observe low probability of sphalerite transforming into NaCl at the low energy lids, but with an increase of energy, the probability increases.

5. Conclusion

We performed a structure prediction study for bulk PbS at different pressures using ab initio energy calculations during both the global search and the local optimization. Our calculations are in good agreement with experimental results [32–35], and we predict new modifications [36]. Furthermore, a global optimization in the ZnO system was performed with an empirical potential for a number of different pressures, followed by refinement on ab initio level. Again good agreement with experimental [40] and theoretical results [52] was found, including the identification of a new interesting modification [42, 43]. In addition, threshold and prescribed path runs were performed, in order to generate 2-D-representations of the energy landscape of the ZnO.

References

[1] J.C. Schön, M. Jansen, *Angew. Chem., Int. Ed. Eng.* **35**, 1286 (1996).

[2] P. Verwer, F. J. J. Leusen, *Rew. Comp. Chem.* **12**, 327 (1998).

[3] C. Mellot Draznieks, J.M. Newsam, A.M. Gorman, C.M. Freeman, G. Férey, *Angew. Chem., Int. Ed. Eng.* **39**, 2275 (2000).

[4] M. Jansen, *Angew. Chem., Int. Ed Eng.* **41**, 3746 (2002).

[5] J.C. Schön, M. Jansen, *Mater. Res. Soc. Symp. Proc.* **848**, (2005).

[6] S. L. Price, *Phys. Chem. Chem. Phys.* **10**, 1996 (2008).

[7] S.M. Woodley, C.R.A. Catlow, *Nature Mater.* **7**, 937 (2008).

[8] J.C. Schön, M. Jansen, *Int. J. Mat. Res.* **2**, 135 (2009).

[9] J.C. Schön, K. Doll, M. Jansen, *phys. stat. sol.* **B247**, 23 (2010).

[10] M. Jansen, K.Doll, J.C. Schön, *Acta Cryst.* **A66**, 518 (2010).

[11] D.J. Wales, *Energy Landscapes*, Cambridge University Press, Cambridge 2003.

[12] C.R.A. Catlow, J.M. Thomas, C.M. Freeman, P.A. Wright, R.G. Bell, *Proc. Roy. Soc.* **A442**, 85 (1993).

[13] A.R. Oganov, S. Ono, *Nature*, **430**, 445 (2004).

[14] J.C. Schön, I.V. Pentin, M. Jansen, *Phys. Chem. Chem. Phys.* **8**, 1778 (2006).

[15] J.C. Schön , Z.P. Cancarevic, M. Jansen, *J. Chem. Phys.* **121**, 2289 (2004).

[16] M.A.C. Wevers, J.C. Schön, M. Jansen, *J. Solid State Chem.* **136**, 151 (1998).

[17] J.C. Schön, *ZAAC* **630**, 2354 (2004).

[18] J.C. Schön, Z. Cancarevic, A. Hannemann, M. Jansen, *J. Chem. Phys.* **128**, 194712 (2008).

[19] A.R. Oganov, C.W. Glass, *J. Chem. Phys.* **124**, 244704 (2006).

[20] C.J. Pickard, R.J. Needs, *Phys. Rev. B* **76**, 144114 (2007).

[21] K. Doll, J.C. Schön, M. Jansen, *Phys. Chem. Chem. Phys.* **9**, 6128 (2007).

[22] K. Doll, J.C. Schön, M. Jansen, *Phys. Rev. B* **78**, 144110 (2008).

[23] A. Kulkarni, K. Doll, J.C. Schön, M. Jansen, *J. Phys. Chem. B* **47**, 114 (2010).

[24] S. Kirkpatrick, C.D. Gelatt Jr, M.P. Vecchi, *Science* **220**, 671 (1983).

[25] J.C. Schön, H. Putz, M. Jansen, *J. Phys. Cond. Mattter.* **8**, 143 (1996).

[26] R. Hundt, J.C. Schön, A. Hannemann, M. Jansen, *J. Appl. Cryst.* **32**, 413 (1999).

[27] A. Hannemann, R. Hundt, J.C. Schön, M. Jansen, *J. Appl. Cryst.* **31**, 922 (1998).

[28] R. Hundt, J.C. Schön, M. Jansen, *J. Appl. Cryst.* **39**, 6 (2006).

[29] D. Sheppard, R. Terrell, G. Henkelman, *J. Chem. Phys.* **128**, 134106 (2008).

[30] Xiaofei Liu, Mingde Zhang, *Inter. J. Infrared Millimeter Waves* **21**, 1697 (2000).

[31] Y. Noda, K. Matsumoto, S. Ohba, Y. Saito, K. Toriumi, Y. Iwata, I. Shibuya, *Acta Crystallographica* **C43**, 1443 (1987).

[32] T.K. Chattopadhyay, H.G. von Schnering, W.A. Grosshans, W.B. Holzapfel, *Physica B, C* **139**, 356 (1986).

[33] A.Grzechnik, K.Friese, *J.Phys.Condens.Matter.* **22**, 095402 (2010).

[34] K. Knorr, L. Ehm, B. Winkler, W. Depmeier, *Eur. Phys. J.* **B31**, 297 (2003).

[35] Yu.S. Ponosov, S.V. Ovsyannikov, S.V. Streltsov, V.V. Shchennikov, K. Syassen, *High Pressure Research* **29**, 224 (2009).

[36] D. Zagorac, K. Doll, J.C. Schön, M. Jansen, *Phys. Rev. B*, submitted.

[37] A. Hernandez-Battez, R. González, J.L. Viesca, J.E. Fernández, J.M. Díaz-Fernández, A. Machado, R. Chou, J. Riba, *Wear* **265**, 422 (2008).

[38] H. Sowa, H. Ahsbahs, *J. Appl. Cryst.* **39**, 169 (2006).

[39] S. Cui, W. Feng, H. Hu, Z. Feng, Y. Wang, *J. of Alloys, Compounds* **476**, 306 (2009).

[40] U. Ozgur, Ya.I. Alivov, C. Liu, A. Teke, M.A. Reshchikov, S. Dogan, V. Avrutin, S.-J. Cho, H. Morkoç, *J. Appl. Phys.* **98**, 041301 (2005).

[41] J.C. Schön, M. Jansen, *Comp. Mater. Sci.* **4**, 43 (1995).

[42] C.L. Pueyo, S. Siroky, S. Landsmann, M.W.E. van den Berg, M.R. Wagner, J.S. Reparaz, A. Hoffmann, S. Polarz, *Chem. Mater.* **22**, 4263 (2010).

[43] C. Tusche, H.L.Meyerheim, J. Kirschner, *PRL* **99**, 026102 (2007).

[44] D. Heidrich, W. Kliesch, W. Quapp, *Properties of Chemically Interesting Potential Energy Landscapes*, Springer, Heidelberg 1991.

[45] J.C. Gower, *Biometrika* **53**, 325 (1966).

[46] K.H. Hoffmann, P. Sibani, *Phy. Rev. A* **38**, 4261 (1988).

[47] A. Heuer, *Phys. Rev. Lett.* **78**, 4051 (1997).

[48] T. Komatsuzaki, K. Hoshino, Y. Matsunga, G.J. Rylance, R.L. Johnston, D.J. Wales, *J. Chem. Phys.* **122**, 084714 (2005).

[49] J.P.K. Doye, C.P. Massen, *Cond. Mat.* **1**, 0411144 (2004).

[50] M.H. Trauth, *Matlab — Recipes for Earth Sciences.* Springer, Potsdam 2007.

[51] M.A.C. Wevers, J.C. Schön, M. Jansen, *J. Phys.: Cond. Matter.* **11**, 6487 (1999).

[52] H.Y. Wu, X.L. Cheng, C.H. Hu, P. Zhou, *Physica B* **405**, 606 (2010).